



Xing, L., McKellar, R. C., Xu, X., Li, G., Bai, M., Persons, W. S., ... Currie, P. J. (2016). A Feathered Dinosaur Tail with Primitive Plumage Trapped in Mid-Cretaceous Amber. *Current Biology*, 26(24), 3352-3360.
<https://doi.org/10.1016/j.cub.2016.10.008>

Peer reviewed version

License (if available):
Other

Link to published version (if available):
[10.1016/j.cub.2016.10.008](https://doi.org/10.1016/j.cub.2016.10.008)

[Link to publication record in Explore Bristol Research](#)
PDF-document

This is the accepted author manuscript (AAM). The final published version (version of record) is available online via Elsevier at <http://dx.doi.org/10.1016/j.cub.2016.10.008>. Please refer to any applicable terms of use of the publisher.

University of Bristol - Explore Bristol Research

General rights

This document is made available in accordance with publisher policies. Please cite only the published version using the reference above. Full terms of use are available:
<http://www.bristol.ac.uk/pure/about/ebr-terms>

1 **Current Biology Report**

2 **Title: A feathered dinosaur tail with primitive plumage trapped in mid-Cretaceous amber**

3

4 **Authors:** Lida Xing^{1,2*†}, Ryan C. McKellar^{3,4*†}, Xing Xu^{5†}, Gang Li^{6†}, Ming Bai^{7†}, W. Scott
5 Persons IV⁸, Tetsuto Miyashita⁸, Michael J. Benton⁹, Jianping Zhang², Alexander P. Wolfe⁸,
6 Qiru Yi⁶, Kuowei Tseng¹⁰, Hao Ran¹¹, Philip J. Currie⁸

7

8 **Affiliations:**

9 ¹ State Key Laboratory of Biogeology and Environmental Geology, China University of Geosciences, Beijing
10 100083, China

11 ² School of the Earth Sciences and Resources, China University of Geosciences, Beijing, 100083, China.

12 ³ Royal Saskatchewan Museum, Regina, Saskatchewan, S4P 4W7, Canada.

13 ⁴ Biology Department, University of Regina, Regina, Saskatchewan, S4S 0A2, Canada.

14 ⁵ Key Laboratory of Vertebrate Evolution and Human Origins, Institute of Vertebrate Paleontology and
15 Paleoanthropology, Chinese Academy of Sciences, Beijing 100044, China.

16 ⁶ Institute of High Energy Physics, Chinese Academy of Science, Beijing 100049, China.

17 ⁷ Key Laboratory of Zoological Systematics and Evolution, Institute of Zoology, Chinese Academy of Sciences,
18 Beijing, 100101, China.

19 ⁸ Department of Biological Sciences, University of Alberta, Edmonton, Alberta, T6G 2E9, Canada.

20 ⁹ School of Earth Sciences, University of Bristol, Bristol, BS8 1RJ, UK

21 ¹⁰ Department of Exercise and Health Science, University of Taipei, Taipei 11153, China.

22 ¹¹ Key Laboratory of Ecology of Rare and Endangered Species and Environmental Protection, Ministry of
23 Education, Guilin 541004, China.

24

25

26 * **Contact information:** xinglida@gmail.com (L.X.); ryan.mckellar@gov.sk.ca (R.C.M., lead contact).

27

28 † These authors contributed equally to this work.

29

30

31 **Summary.** In the two decades since the discovery of feathered dinosaurs [1–3], the range of
32 plumage known from non-avian theropods has expanded significantly, confirming several
33 features predicted by developmentally informed models of feather evolution [4–10]. However,
34 three-dimensional feather morphology and evolutionary patterns remain difficult to interpret, due
35 to compression in sedimentary rocks [9,11]. Recent discoveries in Cretaceous amber from
36 Canada, France, Japan, Lebanon, Myanmar, and the USA [12–18] reveal much finer levels of
37 structural detail, but taxonomic placement is uncertain because plumage is rarely associated with
38 identifiable skeletal material [14]. Here we describe the feathered tail of a non-avian theropod
39 preserved in mid-Cretaceous (~99 Ma) amber from Kachin State, Myanmar [17], with plumage
40 structure that informs directly the evolutionary developmental pathway of feathers. This
41 specimen provides an opportunity to document pristine feathers in direct association with a
42 putative juvenile coelurosaur, preserving fine morphological details, including the spatial
43 arrangement of follicles and feathers on the body, and micrometre-scale features of the plumage.
44 Many feathers exhibit a short, slender rachis with alternating barbs and a uniform series of
45 contiguous barbules, supporting the developmental hypothesis that barbs already possessed
46 barbules when they fused to form the rachis [19]. Beneath the feathers, carbonized soft tissues
47 offer a glimpse of preservational potential and history for the inclusion; abundant Fe²⁺ suggests
48 vestiges of primary haemoglobin and ferritin remain trapped within the tail. The new find
49 highlights the unique preservation potential of amber for understanding the morphology and
50 evolution of coelurosaurian integumentary structures.

51

52 **Keywords:** Coelurosauria; feather evolution; Burmese amber; Cenomanian

53

54 **Results and Discussion:**

55 **Preservation.** The tail within DIP-V-15103 is visible to the naked eye as an elongate and gently
56 curved structure (length = 36.73 mm). A dense covering of feathers protrudes from the tail,
57 obscuring underlying details, so Synchrotron Radiation (SR) X-ray phase contrast μ CT scanning
58 was employed to examine concealed osteological and soft tissue features (Figure 1). Soft
59 tissues—presumably muscles, ligaments, and skin—are visible sporadically through the
60 plumage, clinging to the bones in a manner suggestive of the desiccation common to other

61 vertebrate remains in amber [20]. These tissues have largely been reduced to a carbon film,
62 retaining only traces of their original chemical composition. Based on analyses further described
63 in the Supplemental Information, SR μ -XFI shows iron is present in the carbonized soft tissues,
64 and as a series of fine linear features corresponding to exposed plumage (Figure 2). Copper is
65 slightly more abundant in amber containing plumage, but this signal is cryptic and not a clear
66 indicator for preserved pigments. Elements such as Ca, Sc, Zn, Ti, Ge, Mn appear associated
67 with clay minerals filling voids in the amber. We derived the valence state of iron in the sample
68 qualitatively by comparison to the standard XAS of Fe foil, Fe₂O₃, Fe₃O₄, and FeO. Our
69 calculations indicate that more than 80% of iron in the sample is ferrous (Fe²⁺). Similar
70 measurements have been made on vessels preserved within *Tyrannosaurus* and
71 *Brachylophosaurus* bones, and interpreted as indicating the presence of goethite and biogenic
72 iron oxides produced from haemoglobin decomposition [21]. The presence of large quantities of
73 Fe²⁺ in DIP-V-15103 suggests that some primary iron from haemoglobin or ferritin remains
74 trapped within the inclusion. SEM analyses show pyrite (FeS₂) is also present, but not as a
75 significant contributor to the distribution of iron within the specimen (Figure S3).

76 The close contact between the skin and surrounding amber, paired with the mummified
77 external appearance of the skin where it has shriveled across the surface of the vertebrae, suggest
78 one of two scenarios. Either the tail-bearer was dead and partially desiccated before
79 encapsulation, or rapidly dried due to resin interactions. Early-stage drying is further supported
80 by the limited amount of cloudy amber surrounding the tail (Figures 1C, S2), which is a
81 preservational feature related to decay products or moisture interacting with resin [22]. However,
82 drying and resin impregnation were not sufficient to preserve cellular detail in the soft tissues.
83 Based on the clays observed where bone breaches the amber surface, skeletal material was likely
84 exposed on the surface after resin polymerization. The bone has been partially dissolved and
85 infilled with clay from the surrounding matrix [17], much like insect body cavities in this deposit
86 (Figure S2A). Presence of Fe²⁺ within the carbonized remains suggests that organic components
87 were trapped early and remained undisturbed by subsequent events. Further taphonomic
88 constraints are difficult to infer. It is unclear whether the lack of melanosomes within the keratin
89 sheets of the surrounding feathers (Figures 2B, S3) might provide additional taphonomic
90 information, or if their absence results from weakly pigmented feathers or the small sample area
91 available for SEM analyses. Artificial maturation experiments [23] have shown the breakdown of

92 modern melanosomes at a range of temperatures, but this work was conducted at temperatures
93 that would also degrade amber. The taphonomic pathway that led to the preservation of DIP-V-
94 15103 is not entirely clear, but it suggests promise for more detailed examinations of organics or
95 pigmentation in vertebrate inclusions.

96

97 **Osteology.** SR X-ray μ CT scanning of DIP-V-15103 (Figure 1) revealed that soft tissues have a
98 density insufficiently different from the partially replaced skeletal elements to permit X-ray
99 imaging and virtual dissection of osteology alone. Consequently, many diagnostic and
100 comparative osteological details remain obscured. However, two vertebrae are clearly delineated
101 ventrally (Figure 1F–H). Extrapolating lengths of these vertebrae, the preserved tail section
102 contains at least eight full vertebrae and part of a ninth. The vertebrae are elongate, with
103 anteroposterior lengths double the maximum diameter of the tail (Supplemental Table 1).
104 Vertebral proportions and tail flexion preclude membership within the Pygostylia [*sensu* 24].
105 Even with the skin adpressed to the bony surface, no features other than the grooved ventral sulci
106 of two centra are clearly visible. This lack of topography suggests that the vertebrae lack
107 prominent neural arches, transverse processes, or haemal arches. Therefore, the preserved
108 segment is only a small mid to distal portion of what was likely a relatively long tail, with the
109 total caudal vertebral count not reasonably less than fifteen, and likely greater than twenty-five.
110 Based on specimen size, it also seems likely that the tail belonged to a juvenile.

111 DIP-V-15103 is interpreted as a non-avian coelurosaur tail: its vertebral profiles and
112 estimated length rule out avebrevicaudan birds, oviraptorosaurs, and scansoriopterygians—
113 lineages generally characterized by a short caudal series with subequal centra [25–27], with the
114 exception of *Epidendrosaurus*. The branched feathers have a weak pennaceous arrangement of
115 barbs consistent with non-avian coelurosaurs, particularly paravians. Although the feathers are
116 somewhat pennaceous, none of the observed osteological features preclude a compsognathid [28]
117 affinity. The presence of pennaceous feathers in pairs down the length of the tail may point
118 toward a source within Pennaraptora [9], placing a lower limit on the specimen’s phylogenetic
119 position. However, the distribution and shape of the feathers only strongly supports placement
120 crownward of basal coelurosaurs, such as tyrannosaurids and compsognathids. In terms of an
121 upper limit, the specimen can be confidently excluded from Pygostylia; and it can likely be
122 excluded from the long-tailed birds, based on pronounced ventral grooves on the vertebral

123 centra. Additional taxonomic assessment details are provided in Supplemental Information.

124

125 **Plumage.** Both SR X-ray μ CT reconstruction and standard light microscopy confirm feather
126 attachments throughout the preserved tail length (Figure 1). A bilaterally paired series of
127 posterodorsally oriented feathers extends from the dorsal midline (Figure 1D,E). Another row of
128 feathers is present at mid-height on each side of the tail, with feathers extending posterolaterally
129 at roughly 45° to its long axis (Figure 1D–G). These follicle pairs appear evenly spaced along the
130 length of the tail. Where the outlines of two vertebral centra are visible, follicles are located at
131 the mid-lengths of centra and at intervertebral joints. Ventral plumage is sparse, consisting of fine
132 feathers that follow the long axis of the tail closely (Figure 1 B,G,H). Overall, the plumage forms
133 laterally directed keels on either side of the vertebral column, providing a unique opportunity to
134 observe feather counts and orientations within the contour-like caudal plumage of a coelurosaur.
135 DIP-V-15103 does not show the splaying of large pennaceous rectrices observed alongside the
136 posteriormost caudals of long-tailed birds [29]. Either splaying was absent in this individual, or
137 only present caudally, beyond the preserved region. Nevertheless, the arrangement of feathers
138 into lateral keels in DIP-V-15103 is similar to the paravian tail fan or frond [9]. Such
139 arrangements, composed of different feather types, can occur not just at the distal tip but also
140 along the entire length of the tail. Amber preservation suggests that the tail fans and fronds
141 preserved in paravians are not merely a taphonomic artefact of compression.

142 If DIP-V-15103 indeed represents a juvenile coelurosaur tail, the feathers most likely
143 characterize adult plumage—however there is some room for uncertainty. Basal taxa within
144 Pennaraptora, such as *Similicaudipteryx*, are thought to have undergone dramatic moults that
145 affected the tail region [8], meanwhile some basal members of Pygostylia have precocial
146 juveniles with adult-like plumage [14]. The pennaceous feathers and barbules of DIP-V-15103
147 suggests an adult-like plumage, where feathers would not have been replaced by different
148 morphotypes in subsequent moults. Alternatively, the feather-bearer may not have conformed to
149 the moult patterns found in modern birds.

150 The feathers of DIP-V-15103 are similar to each other in morphology, regardless of position
151 on the tail (Figures 3, S4). All preserved feathers have a weakly defined rachis that is nearly
152 indistinguishable from the barb rami apically, and slightly thickened basally (Figure 3). Both
153 rachises and barbs are sub-cylindrical in cross section. Although the rachis thickens basally, the

154 maximum diameter near the follicle is approximately three times that of an adjacent barb ramus
155 (Figures 3, S4). Feathers near the anterior end of the dorsal series have the greatest basal
156 expansion observed among the plumage, with rachis widths approaching 60 μm (Figures 3,
157 4A,B). Rachises among these feathers become as narrow as 18 μm in apical positions, while barb
158 rami have widths ranging from 15 to 23 μm . Within individual feathers, barbs are positioned
159 alternately along the rachis, approaching an opposite arrangement basally, with wide spacing
160 between, and a weak planar arrangement (Figure 4). Flexion within the amber indicates barb
161 rami were flexible, and the rachis itself was somewhat flexible. The open, flexible structure of
162 these feathers is more analogous to modern ornamental feathers than to flight feathers, showing
163 structural similarities to the distal components of contour feathers in certain Anseriformes
164 (Figures 3, S5). The paired feather arrangement is similar to rectrices in modern birds,
165 suggesting that tracts had become established in basal tail plumage before pygostyle
166 development, with tail plumage becoming more specialized over time. If the entire tail bore
167 plumage similar to that trapped in DIP-V-15103, the feather-bearer would likely have been
168 incapable of flight.

169 The feathers of DIP-V-15103 display exquisitely preserved barbules. Strikingly, the simple
170 barbules branch not only within individual barbs but also unmodified from the rachis (Figures 3;
171 4; S4G,H). In this regard, the feathers are comparable to the contours of many modern birds,
172 which also possess some barbules that originate from the rachis (rachidial barbules), although
173 usually from the proximal barb base and in reduced form. In DIP-V-15103, barbules branch in an
174 evenly spaced, paired, and nearly symmetrical manner. This pattern remains consistent in both
175 proximal and distal barbules, from proximal to distal barbs, and along the rachis. Barbules are
176 consistently blade-shaped, with pigmentation outlining five basal cells followed by a poorly
177 differentiated pennulum lacking discernible nodes or nodal protrusions (Figure 3E–H). Close
178 spacing between barbules, combined with the orientation of their flattened surfaces (parallel to
179 the feather's long axis), yields open-vaned feathers that are largely pennaceous.

180 The weakly developed rachis and contiguous barbule branching in DIP-V-15103 represents
181 a novel combination among theropods. Within the evolutionary developmental model of feathers
182 [5], DIP-V-15103 appears intermediate between stages IIIa (rachis with naked barbs) and IIIb
183 (barbs with barbules, lacking a rachis), but does not exactly fit Stage IIIa+b (rachis with barbs
184 bearing barbules) (Figure 4C). In DIP-V-15103, barbs exhibit an alternating arrangement along a

185 poorly defined rachis, with nearly dichotomous branching apically, and barbules continue along
186 the surface of the rachis and barbs. The weakly developed rachis appears to have formed through
187 fusion of individual barbs that already possessed barbules (Stage IIIb), instead of fusion of naked
188 barbs (Stage IIIa) [5]. The barb branching pattern continues largely uninterrupted toward the
189 follicle, as do the pervasive, undifferentiated barbules. Unless the condition observed in DIP-V-
190 15103 represents a secondary reduction of the rachis, the evolutionary pathway for feathers in
191 this coelurosaur may have been through Stage IIIb (barbs with barbules), not Stage IIIa (fusion
192 of naked barbs). Cytological observations of barbule development along the barb vane ridge
193 support the evolutionary coupling of barbs and barbules [19,30]. Feather morphology of DIP-V-
194 15103 contrasts with the reduced rachis and long, naked, filamentous barbs in the branched
195 caudal plumage of the dromaeosaurid *Sinornithosaurus* [6,8] and the therizinosauroid
196 *Beipiaosaurus* [31]. This either suggests a greater diversity of tail plumage in coelurosaurians
197 than previously suspected, or a simplified form of more derived pennaceous feathers in DIP-V-
198 15103.

199 The unusual barbule configuration in DIP-V-15103 suggests that barbules were primitively
200 distributed evenly throughout the length of the feather and only later became restricted to the
201 barbs and proximal rachis and oriented so that their edges face the feather surfaces, as in modern
202 avians. In modern birds, barbule cells originate in the subperiderm and merge into a syncytium
203 on either side of the barb vane ridge [32,33]. The symmetrical arrangement of barbules along the
204 barbs in DIP-V-15103 implies symmetry of barbule cells across the barb vane ridge. The
205 contiguous barbule branching along the rachis probably occurs along the barb vane ridge leading
206 to the apicalmost barb. In the lineage leading to birds, the barbules became spatially restricted to
207 the barbs and the proximal portion of the rachis, presumably to accommodate increasing barb
208 number and density related to rigid pennaceous feathers (Stage IIIa+b and/or IV) [5].
209 Alternatively, the barbule pattern in DIP-V-15103 may represent a highly derived and potentially
210 experimental character state unrelated to the avian lineage. Whichever the case, DIP-V-15103
211 suggests that non-avian theropods had a greater variety of feather forms than predicted from
212 developmental phenotypes in modern feathers [4,5,10].

213 Traces of pigmentation exist within the entombed plumage. Discrete bands corresponding to
214 basal cells within each barbule are visible due to loosely confined pigments (Figure 3C–H).
215 Pigmentation is more pronounced within apical portions of each barbule, and in the barb rami

216 and rachis of dorsal feathers (Figures 1C, S4H). Coloration varies little within individual
217 feathers, but dorsal plumage is significantly darker than ventral plumage. Preserved coloration
218 suggests a chestnut brown dorsal surface, contrasting against pale or almost white ventral
219 plumage (Figures 1A–C, S4A–D); however, taphonomic impacts on visible colors are unclear. A
220 small section of the pale ventral plumage was available for SEM observations. No melanosomes
221 were observed, suggesting ventral plumage was either unpigmented or pigmented through
222 alternative means, such as carotenoids [34]. Keratin sheets are visible within the feather layer,
223 displaying the distinctive, porous, laminar structure also observed in modern avian barbules
224 under SEM (Figure S2A,B).

225 The theropod tail reported here is an astonishing fossil, highlighting the unique preservation
226 potential of amber. Importantly, in the context of bird origins, feathers and flight are key
227 elements contributing to the success of the clade. Recent finds from Asia [1–4,6,8–11] have
228 revealed unexpected diversity in feather morphologies and flight modes among the proliferation
229 of small Jurassic–Cretaceous theropods near the origin of birds with powered flight. DIP-V-
230 15103 adds another morphotype to this diversity. The integration of developmental studies
231 [5,7,33] and paleontology yields enriched models of morphological character evolution that help
232 explain major evolutionary transitions in key clades such as theropods, including birds. With
233 preservation in amber, the finest details of feathers are visible in three-dimensions, providing
234 concrete evidence for feather morphologies and arrangement upon the tail, and supporting an
235 important role for barbs and barbules in feather evolution.

236

237 **Experimental Procedures:**

238 DIP-V-15103 was imaged and observed using propagation phase contrast Synchrotron Radiation
239 X-ray microtomography (PPC-SR X-ray μ CT); standard microscopy, micro- and
240 macrophotography (including transmitted, incident, dark field, and UV lighting); and scanning
241 electron microscopy (SEM). Chemical composition was analyzed using Synchrotron Radiation
242 micro-X-ray fluorescence imaging (μ -XFI), and X-ray absorption spectroscopy (XAS). Full
243 details of experimental procedures for imaging and chemical analyses are provided in
244 Supplemental Experimental Procedures. Feather morphological terms follow [5] and [35], while
245 pigmentation terminology follows [36]. Institutional abbreviations include DIP (Dexu Institute of

246 Palaeontology, Chaozhou, China); RSM (Royal Saskatchewan Museum, Regina, Canada).
247 Specimen measurements are based on ocular micrometer readings, or 3-D reconstructions (with
248 commentary).

249

250 **Author Contributions:**

251 L.X., R.M.: project design, leadership, funding, visualization, writing; X.X., W.P., T.M., P.C.:
252 morphological analysis, editing; G.L., M.B., Q.Y.: 3D modeling, elemental analysis, editing;
253 K.T.: taphonomic analysis; M.J.B., H.R.: data and CT model analysis, editing; J.Z.: geological
254 background; A.W.: SEM analysis, editing.

255 **Acknowledgments:** We thank Chinese Academy of Science (YZ201211, BASIC 2014-01),
256 National Science Fund of China (NSFC-J1210002), Shaanxi Province (No. 2013-19),
257 National Geographic Society, USA (EC0768-15), National Sciences Engineering
258 Research Council, Canada (2015-00681), and Humboldt Fellowship for support; Beijing
259 Synchrotron Radiation Facility (BSRF) and Shanghai Synchrotron Radiation Facility
260 (SSRF) for beamtime; staffs of 4W1A and B of BSRF, and 13W of SSRF, for analytical
261 assistance; Zhao Haifei, Zhang Jie, An Pengfei and Wang Yanping of BSRF for research
262 assistance; Ray Poulin (RSM) for discussions; and Nathan Gerein (University of Alberta)
263 for SEM assistance.

264

265 **References:**

- 266 1. Ji, Q., and Ji, S-A. (1996). On the discovery of the earliest fossil bird in China
267 (*Sinosauropteryx* gen. nov.) and the origin of birds. *Chin. Geol.* 233, 30–33.
- 268 2. Ji, Q., Currie, P.J., Norell, M.A., and Ji, S. (1998). Two feathered dinosaurs from
269 northeastern China. *Nature* 393, 753–761.
- 270 3. Chen, P.J., Dong, Z.M., and Zhen, S.N. (1998). An exceptionally well-preserved theropod
271 dinosaur from the Yixian Formation of China. *Nature* 391, 147–152.
- 272 4. O'Connor, J.K., Chiappe, L.M., Chuong, C., Bottjer, D.J., and You, H. (2012) Homology and
273 potential cellular and molecular mechanisms for the development of unique feather
274 morphologies in early birds. *Geosciences* 2, 157–177.

- 275 5. Prum, R.O. (1999) Development and evolutionary origin of feathers. *J. Exp. Zool.* 285, 291–
276 306.
- 277 6. Xu, X., Zhou, Z., and Prum, R.O. (2001). Branched integumental structures in
278 *Sinornithosaurus* and the origin of feathers. *Nature* 410, 200–204.
- 279 7. Prum, R.O., and Dyck, J. (2003). A hierarchical model of plumage: morphology,
280 development, and evolution. *J. Exp. Zoolog. B Mol. Dev. Evol.* 298B, 73–90.
- 281 8. Xu, X., Zheng, X., and You, H. (2010). Exceptional dinosaur fossils show ontogenetic
282 development of early feathers. *Nature* 464, 1338–1341.
- 283 9. Xu, X., *et al.* (2014). An integrative approach to understanding bird origins. *Science* 346,
284 1253293.
- 285 10. Chen, C.-F., *et al.* (2015). Development, regeneration, and evolution of feathers. *Annu. Rev.*
286 *Anim. Biosci.* 3, 169–195.
- 287 11. Norell, M.A., and Xu, X. (2005). Feathered dinosaurs. *Annu. Rev. Earth. Planet. Sci.* 33,
288 277–299.
- 289 12. McKellar, R.C., Chatterton, B.D.E., Wolfe, A.P., and Currie, P.J. (2011). A diverse
290 assemblage of Late Cretaceous dinosaur and bird feathers from Canadian amber. *Science*
291 333, 1619–1622.
- 292 13. Nascimbene, P.C., Dove, C.J., Grimaldi, D.A., and Schmidt, A.R. (2014). Exceptional
293 preservation of feather microstructures in amber from diverse faunas (Theropoda: Paraves)
294 during the Lower and mid-Cretaceous. 9th European Palaeobotany-Palynology Conference,
295 Pavoda, Italy Abstract Book pp. 113–114.
- 296 14. Xing, L. *et al.* (2016). Mummified precocial bird wings in mid-Cretaceous Burmese amber.
297 *Nat. Comm.* 7(12089), doi: 10.1038/ncomms12089
- 298 15. Schlee, D., and Glöckner, W. (1978). Bernstein: Bernsteine und Bernstein-Fossilien. *Stuttg.*
299 *Beitr. Naturkd. C* 8, 1–72.
- 300 16. Grimaldi, D.A., and Case, G.R. (1995). A feather in amber from the Upper Cretaceous of
301 New Jersey. *Am. Mus. Novit.* 3126, 1–6.
- 302 17. Grimaldi, D.A., Engel, M.S., and Nascimbene, P.C. (2002). Fossiliferous Cretaceous amber
303 from Myanmar (Burma): its rediscovery, biotic diversity, and paleontological significance.
304 *Am. Mus. Novit.* 3361, 1–72.
- 305 18. Perrichot, P., Marion, L., Néraudeau, D., Vullo, R., and Tafforeau, P. (2008). The early

- 306 evolution of feathers: fossil evidence from Cretaceous amber of France. Proc. R. Soc. B 275,
307 1197–1202.
- 308 19. Alibardi, L. (2006). Cells of embryonic and regenerating germinal layers within barb ridges:
309 implication for the development, evolution and diversification of feathers. J. Submicrosc.
310 Cytol. Pathol. 38, 51–76.
- 311 20. De Queiroz, K., Chu, L.-R., and Losos, J.B. (1998) A second *Anolis* lizard in Dominican
312 amber and the systematics and ecological morphology of Dominican amber anoles. Am.
313 Mus. Novit. 3249, 1–23.
- 314 21. Schweitzer, M.H., *et al.* (2014). A role for iron and oxygen chemistry in preserving soft
315 tissues, cells and molecules in deep time. Proc. R. Soc. B 281, 20132741.
- 316 22. Grimaldi, D.A., and Engel, M.S. (2005). Evolution of the Insects (Cambridge Univ. Press).
- 317 23. Colleary, C. *et al.* (2015). Chemical, experimental, and morphological evidence for
318 diagenetically altered melanin in exceptionally preserved fossils. PNAS 112(41), 12592–
319 12597.
- 320 24. O’Connor, J.K., Wang X., Zheng X., Hu H., Zhang X., and Zhou Z. (2016). An
321 enantiornithine with a fan-shaped tail, and the evolution of the rectricial complex in early
322 birds. Current Biol. 26(1), 114-119.
- 323 25. Zhang, F., Zhou, Z., Xu, X., Wang, X., and Sullivan, C. (2008) A bizarre Jurassic
324 maniraptoran from China with elongate ribbon-like feathers. Nature 455, 1105–1108.
- 325 26. O’Connor, J.K., and Zhou, Z. (2013). A redescription of *Chaoyangia beishanensis* (Aves)
326 and a comprehensive phylogeny of Mesozoic birds. J. Syst. Palaeontol. 11, 889–906.
- 327 27. Persons, W.S., Currie, P.J., and Norell, M.A. (2013). Oviraptorosaur tail forms and functions.
328 Acta Palaeontol. Pol. 59, 553–567.
- 329 28. Currie, P.J., and Chen, P. (2001). Anatomy of *Sinosauroptryx prima* from Liaoning,
330 northeastern China. Can. J. Earth Sci. 38, 1705–1727.
- 331 29. O’Connor, J.K., Sun, C., Xu, X., Wang, X., and Zhou, Z. (2012). A new species of *Jeholornis*
332 with complete caudal integument. Hist. Biol. 24, 29–41.
- 333 30. Alibardi, L., and Sawyer, R.H. (2006). Cell structure of developing downfeathers in the
334 zebrafinch with emphasis on barb ridge morphogenesis. J. Anat. 208, 621–642.
- 335 31. Xu, X., Tang, Z., and Wang, X. (1999). A therizinosauroid dinosaur with integumentary
336 structures from China. Nature 399, 350.

- 337 32. Alibardi, L. (2005). Cell structure of developing barbs and barbules in downfeathers of the
338 chick: central role of barb ridge morphogenesis for the evolution of feathers. *J. Submicrosc.*
339 *Cytol. Pathol.* 37, 19–41.
- 340 33. Alibardi, L. (2007). Cell interactions in barb ridges of developing chick downfeather and the
341 origin of feather branching. *Ital. J. Zool.* 74, 143–155.
- 342 34. Thomas, D.B., Nascimbene, P.C., Dove, C.J., Grimaldi, D.A., and James, H.F. (2014).
343 Seeking carotenoid pigments in amber-preserved fossil feathers. *Sci. Rep.* 4,
344 10.1038/srep05226.
- 345 35. Lucas, A.M., and Stettenheim, P.R. (1979). *Avian Anatomy: Integument* (Washington: US
346 Gov. Printing Office).
- 347 36. Dove, C.J. (2000). A descriptive and phylogenetic analysis of plumulaceous feather
348 characters in Charadriiformes. *Ornithol. Monogr.* 51, 1–163.

349

350

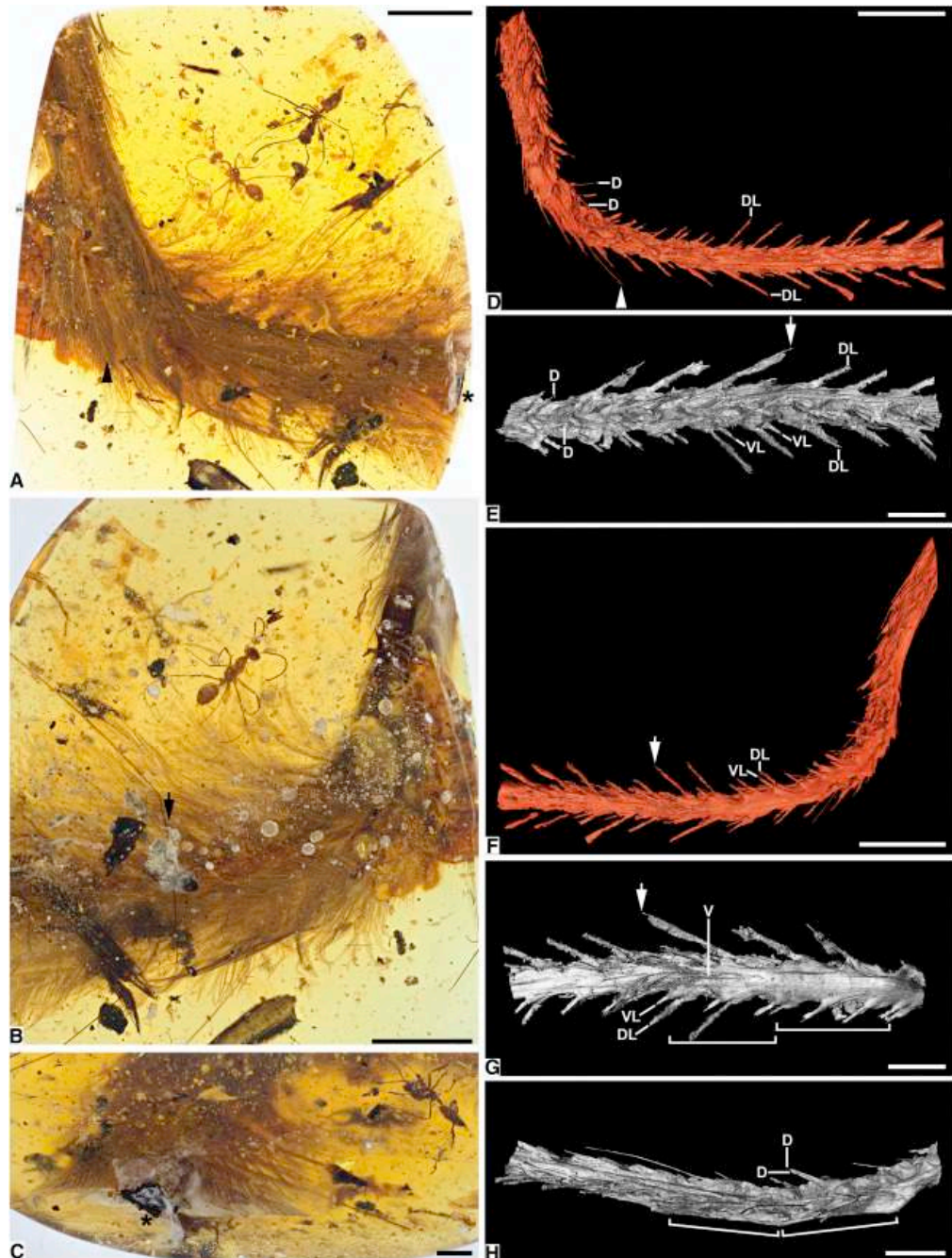
351 **Figure 1.** Photomicrographs and SR X-ray μ CT reconstructions of DIP-V-15103. **(A)**
 352 Dorsolateral overview. **(B)** Ventrolateral overview with decay products (bubbles in foreground,
 353 staining to lower right). **(C)** Caudal exposure of tail, showing darker dorsal plumage (top), milky
 354 amber, exposed carbon film around vertebrae (center). **(D–H)** Reconstructions focussing on
 355 dorsolateral, detailed dorsal, ventrolateral, detailed ventral, and detailed dorsal aspects of tail,
 356 respectively. Arrowheads in (A), (D) mark rachis of feather featured in Figure 4A. Asterisks in
 357 (A) and (C) indicate carbonized film (soft tissue) exposure. Arrows in (B), (E–G) indicate shared
 358 landmark, plus

359 bubbles
 360 exaggerating rachis
 361 dimensions;
 362 brackets in (G) and
 363 (H) delineate two
 364 vertebrae with
 365 clear transverse
 366 expansion and
 367 curvature of tail at
 368 articulation.

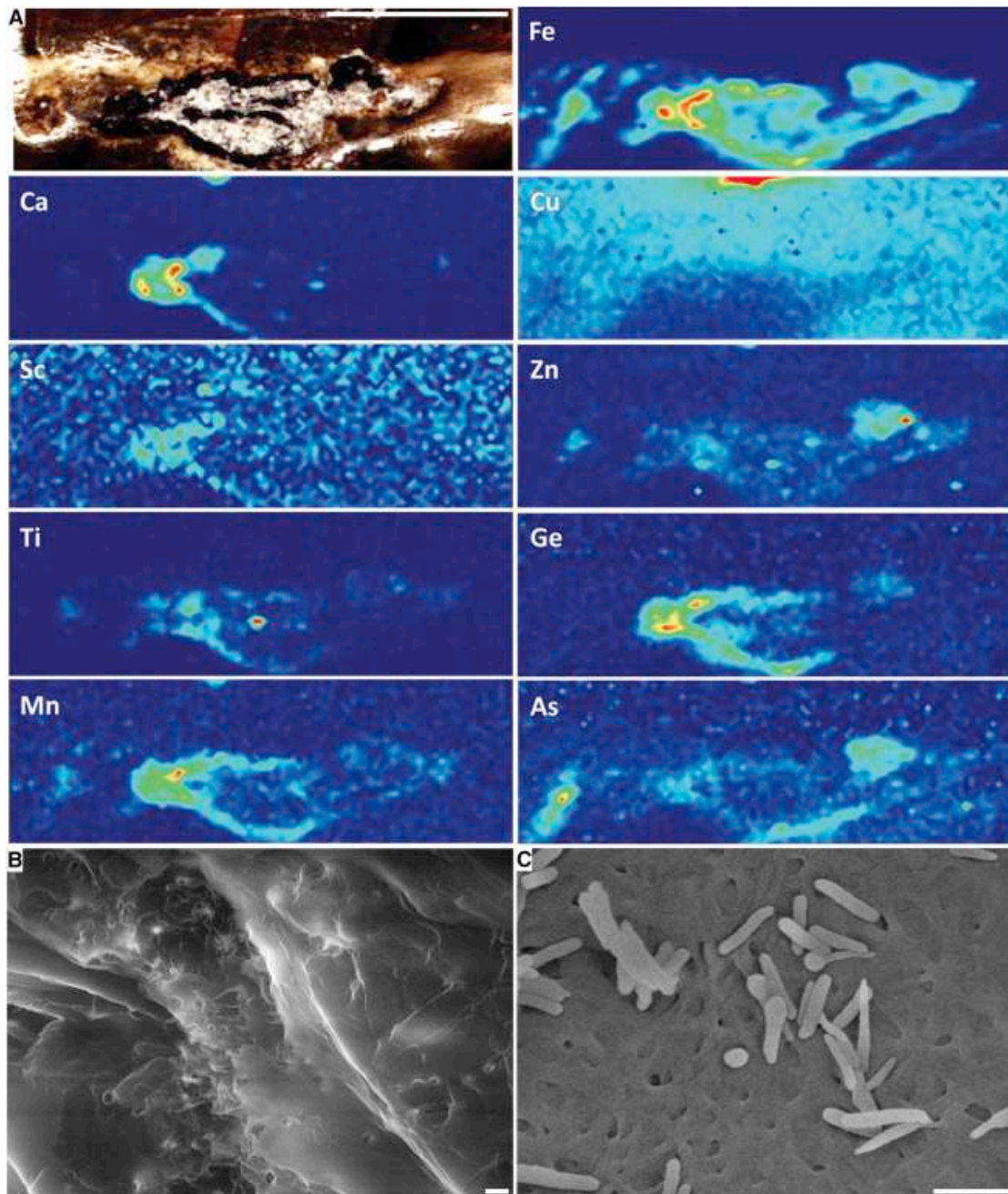
369 Abbreviations for
 370 feather rachises: d,
 371 dorsal; dl,
 372 dorsalmost lateral;
 373 vl, ventralmost
 374 lateral; v, ventral.

375 Scale bars 5 mm in
 376 A,B,D,F; 2 mm in
 377 C,E,G,H. See also
 378 Figure S2.

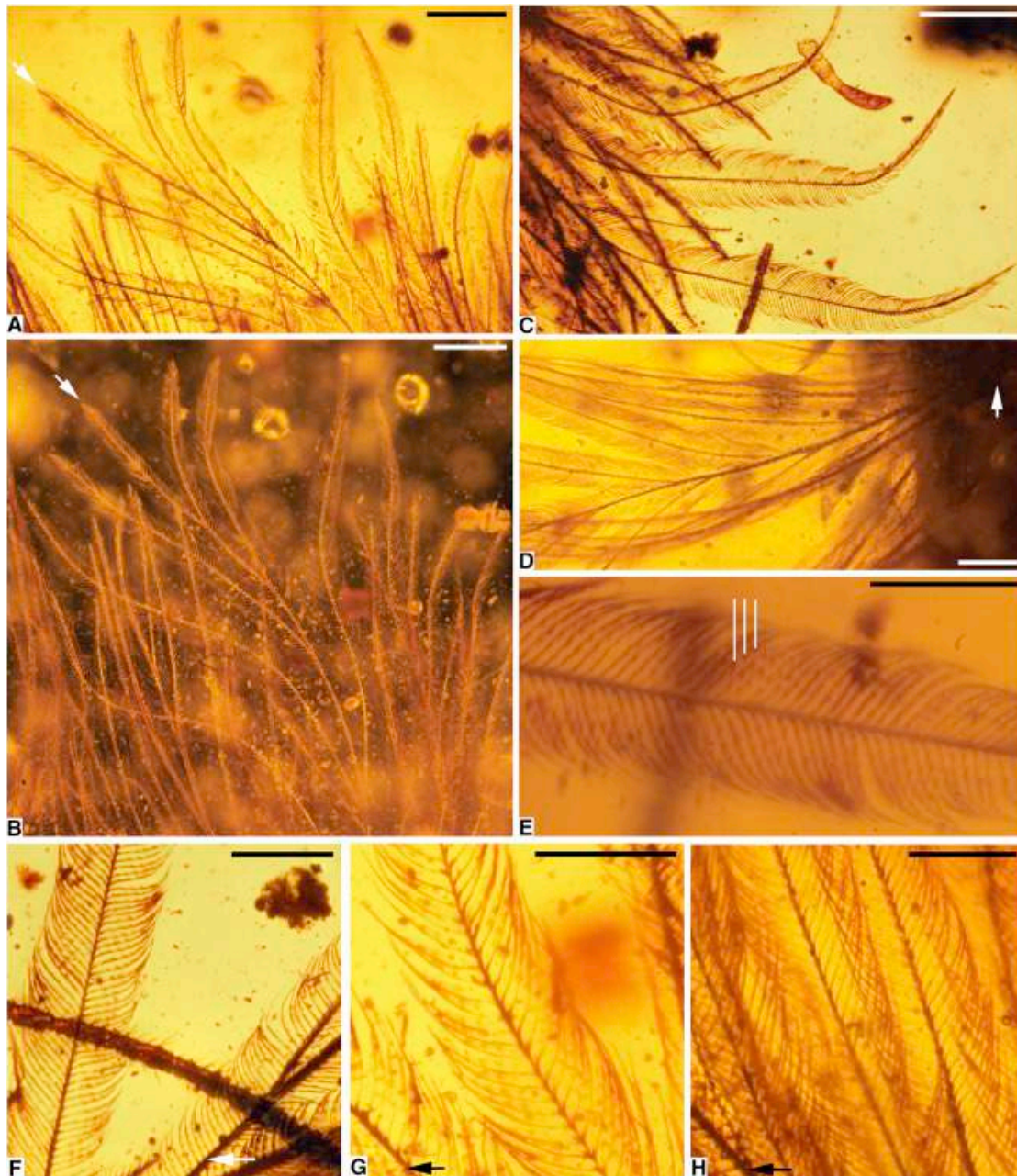
379



380 **Figure 2.** SR μ -XFI maps and scanning electron micrographs of DIP-V-15103. **(A)** Elemental
381 maps and ROI image for exposed soft tissue preservation in DIP-V-15103; black carbon film
382 surrounds clay minerals infilling void between vertebrae or partially replacing them; milky
383 amber related to decay surrounds vertebrae and plumage (ROI prior to clay flake removal better
384 visible in Figure S3H). **(B)** Patchy keratin preservation with traces of fibrous structure in DIP-V-
385 15103 ventral feather. **(C)** Fibrous keratin sheets and isolated melanosomes from barb of modern
386 Indian peafowl (*Pavo cristatus*; Galliformes). Scale bars = 2 mm in A; 1 μ m in B,C. See also
387 Figure S3.



389 **Figure 3.** Photomicrographs of DIP-V-15103 plumage. **(A)** Pale ventral feather in transmitted
 390 light (arrow indicates rachis apex). **(B)** Dark field image of (A), highlighting structure and visible
 391 color. **(C)** Dark dorsal feather in transmitted light, apex toward bottom of image. **(D)** Base of
 392 ventral feather (arrow) with weakly developed rachis. **(E)** Pigment distribution and
 393 microstructure of barbules in (C), with white lines pointing to pigmented regions of barbules. **(F-
 394 H)** Barbule structure variation and pigmentation, among barbs, and ‘rachis’ with rachidial
 395 barbules (near arrows); images from apical, mid-feather, and basal positions respectively. Scale
 396 bars = 1 mm in A, 0.5 mm in B–E, 0.25 mm in F–H. See also Figure S4.



398 **Figure 4.** DIP-V-15103 structural overview, and feather evolutionary-developmental model fit.
 399 **(A,B)** Overview of largest and most planar feather on tail (dorsal series, anterior end), with
 400 matching interpretive diagram of barbs and barbules. Barbules omitted on upper side and on one
 401 barb section (near black arrow) to show rachidial barbules and structure; white arrow indicates
 402 follicle. **(C)** Evolutionary-developmental model and placement of new amber specimen. Brown
 403 = calamus, blue = barb ramus, red = barbule, purple = rachis [after 5, 12]. Scale bars = 1 mm in
 404 A,B.

